Experimental investigation and multi-objective optimization of FDM process parameters for mechanical strength, dimensional accuracy, and cost using a hybrid algorithm

Mohammad Ali Zonoobi[a], **Hamid Haghshenas Gorgani**[b,*], **Dorin Javaherneshan**[c]

[a]Tehran international campus, Sharif University of Technology, Tehran, Iran

[b]Engineering Skills Education Center, Sharif University of Technology, Tehran, Iran

[c]Department of Mechanical Engineering, Aalto University, Espoo, Finland

Abstract

Considering many advantages of 3D printing of polymers using Fused Deposition Modeling (FDM) technique and its service nature, achieving maximum customer satisfaction is very important. The satisfaction of each particular customer may be obtained by providing one or more different outputs of this process, which may not have the same weights. This paper concentrates on multi-objective optimization of three response variables, including tensile strength, dimensional accuracy, and production cost. Eight FDM process parameters containing orientation, layer thickness, infill density, nozzle temperature, print speed, number of shells, infill pattern, and print position have been selected. For carrying out experimental studies, specimens were designed based on Taguchi L27 and manufactured according to ASTM D368-(I) using Polylactic Acid (PLA). Then the signal-to-noise ratio is calculated, and the mathematical regression model of all outputs is obtained. Finally, an intuitive optimal Pareto front is presented to the customer rather than a single point. By repeating the proposed algorithm for eight other customers, the average satisfaction number of 88.56% indicates the efficiency of this method.

Keywords: FDM, Customer Satisfaction, Multi-Objective Optimization, Process Parameters, Design of Experiments

1. Introduction

Additive Manufacturing (AM) is defined as a production method that fabricates objects from Computer Aided Design (CAD) models by creating sequential layers of material [1]. Contrary to traditional processes involving tools and molds, AM uses only the finishing step when necessary; therefore, there is no time and raw materials waist. Fused Deposition Modeling (FDM) is one of the most popular consumer-level AM processes based on extrusion that widely uses thermoplastic filaments, including polycarbonate, Acrylonitrile Butadiene Styrene (ABS), and Polylactic Acid (PLA) [2,3]. Low cost, material flexibility, scalability, and ability to build

*. Corresponding author. Tel.:
E-mail addresses: h_haghshenas@sharif.edu (H. Haghshenas Gorgani); alizonoobi7@gamil.com (M. A. Zonoobi); dorin.javaherneshan@aalto.fi (D. Javaherneshan)

functional parts having complex geometries are the principal reasons for the popularity of this method. In FDM printers, by using a controlled feed mechanism, filament enters a hot cavity, melts into a semi-liquid state, and is extruded through a nozzle. Finally, the created successive two-dimensional layers onto the build platform result in the fabrication of a three-dimensional part [4].

The development of AM technology, along with its application, has increased consumers' expectations and led to a competitive market. Gaining a competitive advantage is crucial in such a market. In this vein, predicting customers' undiscovered needs is an effective way to increase customer satisfaction which will enhance reputation and customer loyalty [5–7]. The same rules apply to companies providing 3D (Three-Dimensional) printing services. Consumers require printed components for various applications, so their definition of quality differs. For instance, if a customer requires stiff parts but cannot afford high-quality products, strength might be decreased to some level to have an optimum production cost. Based on this example, it can be deduced that offering accurately customized services leads to higher customer satisfaction.

In recent years, FDM 3D printers' performance has been improved using various methods. Liu X. *et al.*, in 2017, used gray Taguchi to optimize tensile, flexural, and impact strength [8]. In 2018, Yaman U. *et al.* [9] utilized shrinkage as a tool to compensate for the shrinkage. Printed interior line segments, which are directly connected to the hole perimeter, pull it inward of the artifact. This considerably improves the hole's dimensional accuracy. Raju *et al.*, in 2019, applied a PSO-BFO hybrid method to optimize surface roughness, hardness, tensile strength, and flexural modulus [10]. Akbaş, O. E., *et al.* experimentally and numerically analyzed the effect of the nozzle temperature and feed rates on the dimensions of the FDM polymer parts [11]. According to Menddricky and Fris, in 2020, the height of the layers has the greatest influence on the surface roughness and dimensional accuracy of parts produced by FDM. [12]. In 2021, Dev & Srivastava [13] employed analysis of variance (ANOVA) to investigate the importance of process parameters on flexural strength. In addition, they utilized Response Surface Methodology (RSM) and genetic algorithm to optimize process parameters and achieve favorable flexural strength. In the same year, Camposeco-Negrete [14] investigated the impact of adjustable inputs on processing time, energy consumption, dimensional accuracy, and mechanical properties of the part by applying the Taguchi method besides analysis of variance. The same approach was used by Ramesh & Panneerselvam [15] to determine mechanical characteristics depending on input parameters. As a hybrid method for optimizing dimensional accuracy, Mohamed *et al.* [16] applied a definitive screening design and an artificial neural network. As a different approach, Haghshenas Gorgani *et al.* [17] predicted dimensional errors and modified CAD models with a nonlinear error compensator to improve dimensional accuracy. In 2022, Rezaeian *et al.* investigated the printing speed influence on the mechanical and fractural performance of ABS parts manufactured by the FDM printer [18]. In the same year, Sandhu *et al.* utilized Taguchi orthogonal arrays to study the impact of layer thickness, raster angle, and infill pattern on mechanical properties and surface roughness of FDM parts [19]. In addition, Tosto *et al.* combined FDM and debinding-sintering techniques to reduce the costs of traditional metal AM techniques. They employed the Design Of Experiment technique to study the effect of nozzle temperature, layer thickness, and flow rate on the tensile and bending properties of parts fabricated with this method [20].

As mentioned, most publications related to optimizing FDM process have attempted to identify the effect of input parameters on output responses. Meanwhile, A more efficient use of FDM printers might have been achieved if the behavior of several customer-based response variables were investigated.

Furthermore, in the majority of previous studies, the number of investigated input parameters rarely exceeded six, possibly due to increased calculations or distortion of response functions. In this research, two steps have been taken to solve this problem: First, before the optimization process, a Taguchi analysis is performed, which removes ineffective and noisy data. Second, combining the desirability function with the metaheuristic algorithm of NSGA II reduces the calculations and provides optimal Pareto fronts in 2D (Two-Dimensional) form, which facilitates customer decision-making. In previous research, desirability function and NSGA II have been used alone, but their combination has never been utilized.

Also, in most of the reviewed literature, a single optimal point is presented, which gives only one choice to the beneficiary. However, providing a range of answers as an optimal Pareto front allows the customer to understand various situations intuitively and make a better decision. This leads to greater customer satisfaction which is one of the goals of any service work.

Based on this, the main goals of this research are:

- Defining a response function whose inputs are device settings and outputs are customer requests. Naturally, this function should be a vector function with more than two dimensions.
- Optimizing the response function and providing an optimal Pareto front that gives the customer insight and a wide choice.
- Validation of the method based on conducting tests and measuring its efficiency.

In order to achieve the above goals, firstly the research method is explained in section 2. In section 3, the details of the production and measurement method of the specimens are described, and the results are presented. At the end of this section, the results are analyzed and discussed. Finally, section 4 includes the conclusion, limitations, and suggestions for future research.

2. Materials and methods

Step 1: Identifying inputs and outputs

It is essential to establish significant customer's demands as response variables to gain the highest level of customer satisfaction [21,22]. According to the reviewed literature and customer surveys, tensile strength, dimensional accuracy, and production cost are selected as outputs. The inputs are determined based on highly effective process parameters in slicer software and the most frequent entries in recent years' articles. Accordingly, Orientation, layer thickness, infill density, nozzle temperature, print speed, number of shells, infill pattern, and print position were identified as initial input parameters. It is possible that some of the inputs may be removed due to their negligible or noisy effect.

Step 2: Preparing specimens

Samples are being produced according to ASTM D638-14 (Type I), for both tensile testing, and dimensional measurement. Dimensions of the specimen are indicated in Figure 1. **[Figure 1]**

The full factorial design of experiment method, is very complicated, expensive, and time-consuming [23]. In such a case, the Taguchi orthogonal arrays are very efficient and lead to a significant reduction in the number of experiments [24]. Table 1 provides input parameters' levels, according to available materials, existing printers, and measurement equipment. Figure 2 illustrates the infill pattern types. **[Table 1], [Figure 2]**

According to experiments designed by the Taguchi method in Minitab software, 27 samples should be manufactured as shown in Table 2. **[Table 2]**

Step 3: Measurement of output variables

Calculating the cost of each sample: A stopwatch recorded each sample's printing time, and its mass was measured using a digital scale after production. Accordingly, the cost of each specimen is calculated using Equation (1).

$$C = C_t \times t + C_m \times m \tag{1}$$

Where t indicates the printing time, m is the mass of each specimen, C_t is the price per unit time, and C_m is the price per unit mass.

Measuring the Dimensional Accuracy: The specimens' width was measured by a digital caliper. A lower difference between the width of the CAD model and the actual sample shows higher manufacturing accuracy.

Tensile strength test: An electromechanical universal testing machine was utilized to conduct the tensile test. The ultimate tensile force has been considered as a criterion for comparing samples' strength.

Step 4: Taguchi Analysis:

The results have been analyzed using the Grubbs' test with a significance level of 0.5, and outliers have been removed. Finally, signal-to-noise (S/N) has been obtained using Taguchi analysis where, the chosen strategy is "smaller is better" for dimensional error and price, and "bigger is better" for tensile strength.

Step 5: Obtaining the equation of output responses

RSM is a regression-based statistical approach for obtaining the relation between one or more output responses in terms of several input variables. According to Equation (2), the outputs are generated using "full quadratic regression."

$$Y_i = \sum_{j=1}^{n}\sum_{l=1}^{n} a_i X_j X_l + \sum_{j=1}^{n} b_i X_j + c_i \tag{2}$$

Where Y_i is the output response function, X_j and X_l are input parameters, and a_i and b_i are coefficients. Moreover, i and n are the number of total output responses and input parameters, respectively.

Finally, three distinct equations, including production cost, dimensional error, and tensile strength are obtained and represented by Y_c, Y_a, and Y_s respectively.

Step 6: Optimizing the results

Since the optimization of a vector output function with three components (with respect to three response variables) gives a three-dimensional Pareto front, which may not visually make sense to the end-user [25], the following method is applied:

To begin, each component of tensile strength and dimensional accuracy is weighed between 1 and 10 by the end-user. Suppose these weights are called W_s and W_a respectively. Y_d represents the aggregation of qualitative components in Equation (3):

$$Y_d = (Y_s^{-W_s} Y_a^{W_a})^{(\frac{1}{W_s+W_a})} \tag{3}$$

Note that, ultimately, minimizing Y_d is desirable. The total desirability function is generated from the vector combination of Y_d and Y_c, as shown in Equation (4).

$$F = \begin{bmatrix} Y_d \\ Y_c \end{bmatrix} \tag{4}$$

Then, a multi-objective genetic algorithm (NSGA-ⅠⅠ) on MATLAB software is used to minimize *F*. As a result, a two-dimensional Pareto Front is obtained in which all points represent optimal states. At this stage, the customer can choose one of these points depending on the relative importance of quality and cost.

3. Results and Discussion

3.1. Manufacturing of the specimens and inspection

Samples were fabricated with 1.75 mm diameter PLA filaments on a "Quantum 2025" 3D printer machine. For all samples, the top/bottom solid thickness was 1.08 mm, the nozzle diameter was 0.4 mm, and the bed temperature was 50 ℃. Figures 3 and 4 show specimens being produced and tested; Table 3 provides the main results.

A digital scale with 0.1 g was used to measure each sample's mass. At the time of the study, C_t and C_m in Equation (1) were 0.63 USD/h and 0.02 USD/g, respectively. The dimensional inspection was performed with a digital caliper with 0.01 mm accuracy. Also, tensile testing was conducted on a "ZwickRoell Z100" electromechanical universal testing machine. **[Figure 3 and 4], [Table 3]**

In such samplings, one of the main concerns is the repeatability of the results. Due to the prohibitive expense of making a large number of samples, researchers take one of two approaches [8, 13, 14, 15, 19, and 20]:

One approach is to decrease the number of tests by reducing the number of inputs. Therefore, you can increase repetitions of samples, but the comprehensiveness of the tests faces fundamental doubt due to the reduced number of inputs. Another approach is to maintain the number of inputs and reduce the number of sampling repetitions. In this case, the tests' comprehensiveness is guaranteed, but repeatability is doubtful.

To solve this problem, a modified version of the second approach which involves removing or replacing outlier data using a valid method such as Grubb's test was applied. Two specimens were fabricated for each experiment. Each specimen was dimensionally inspected twice by different individuals. Therefore, the total number of dimensional records is four. Next, by using Grubb's test, the outliers were detected as 18.95, 19.6, and 19.18 in experiments 1, 19, and 21, respectively. To detect outliers in the tensile test results, specimens of each experiment should be compared to each other. However, in this case, there is no criterion to detect an outlier between two data. As an available solution, an initial Taguchi analysis was performed and indicated that the most effective input parameters of tensile strength are infill density and the number of shells. Then, the tensile strength results were categorized into nine groups so that members of each group have the same infill density and number of shells. As a result, the only outlier detected using Grubbs' test was 2172 in experiment 8. No outlier data was observed among the mass and printing time results.

3.2. Taguchi analysis and S/N ratios

Figures 5, 6, and 7 provide the main effects plots for S/N ratio and means of tensile strength, dimensional accuracy, and production cost; furthermore, Tables 4, 5, and 6 represent the responses of S/N ratios to these parameters. The similarity between plots of S/N ratios and means could confirm the validity of the results. The differences are trivial and not decisive. **[Figure 5]**, **[Table 4], [Figure 6], [Table 5], [Figure 7], [Table 6]**

As presented in Table 4 and Figure 5, number of shells and infill density are the most influential parameters in tensile strength. Increasing the infill density and number of shells in the defined range has raised the strength of specimens. They are followed by layer thickness and infill pattern as the next effective parameters. Increasing layer thickness has an inverse effect on the tensile strength. Among the tested infill patterns, the lines pattern makes the toughest specimens. Print position, print speed, nozzle temperature, and orientation have less impact on the printed parts' strength.

According to Table 5, layer thickness, infill density, and orientation have a more noticeable impact on dimensional accuracy than other parameters. As displayed in Figure 6, increasing layer thickness and infill density have put up the dimensional tolerance. Additionally, specimens manufactured with a 45-degree orientation are more accurate. The main effects plots for S/N ratios and means of dimensional accuracy show that print position, nozzle temperature, print speed, number of shells, and infill pattern have minor influences.

Table 6 shows that layer thickness strongly influences production costs. Print speed and infill density stand in the second and third positions, respectively. It is also observed that the number of shells and infill pattern can be neglected. Figure 7 shows that production costs are reduced by thicker layers and faster printing speeds. In addition, increasing infill density leads to more costs. As expected, production costs are unaffected by print position and nozzle temperature. The printing time parameter including nozzle temperature affects production costs in terms of heating.

The comparison of Figures 5 and 7 indicates that number of shells is a dominant parameter for manufacturing a high-strength specimen at a reasonable price.

3.2. Multiple Regression Modeling

According to Section 3, Step 4, RSM has been used to achieve regression models of the output responses. For this, all statistical analyses were carried out in Minitab software.

The full quadratic regression equations for tensile strength, dimensional accuracy, and production cost are presented in Equations (5), (6), and (7). Furthermore, significant P-values have been obtained as the analysis of variance results are presented in Tables 7, 8, and 9, demonstrating the adequacy of regression models corresponding to all three equations. Aside from quadratic regression, linear regression has been performed for tensile strength and production cost. The results show that the quadratic equations are more accurate. For dimensional accuracy, linear and full quadratic led to the same results.

$$Y_s = 1316 - 1456LT - 5.10ID + 292.4NS + 433IP + 0.215ID^2 - 122.6IP^2 + 25.5LT' ID \quad (5)$$

$$Y_a = -0.0606 + 1.028LT + 0.002840ID \quad (6)$$

$$Y_c = 11.3 - 55.43LT + 0.0797 \times ID - 0.2015PS + 0.1338NS + 88.37LT^2 + 0.001266PS^2 - 0.1640LT \times ID + 0.3567LT \times PS - 0.000659ID \times PS \quad (7)$$

As mentioned, Y_a computes dimensional error, therefore its reduction, increases dimensional accuracy. Due to the nature of infill patterns and number of shells, only positive integer values are acceptable for these parameters. **[Table 7-9]**

3.3. Optimization

According to Section 2, Step 6, the customer rates the importance of dimensional accuracy and tensile strength from 1 to 10. In this case study, our customer selected 5 for dimensional accuracy and 9 for tensile strength. Therefore, Equations (3) and (4) are rewritten as Equations (8) and (9), respectively:

$$Y_q = (Y_s^{-9'} Y_a^{5})^{(\frac{1}{9+5})} = Y_s^{-0.64'} Y_a^{0.36} \quad (8)$$

$$F = \begin{bmatrix} Y_s^{-0.64} \times Y_a^{0.36} \\ Y_c \end{bmatrix} \quad (9)$$

Now, the optimization is performed based on the NSGA II algorithm. The result is optimal Pareto front of Figure 8 which contains optimal points. Table 10 coordinates of the points with their corresponding input parameters' values. **[Figure 8], [Table 10]**

There are two problems with the presented Pareto front in Figure 8: first, the customer may not grasp the concept of Y_d, and second, we have calculated Y_c based on our test specimens, whereas the customer's part may differ. The results have been normalized using Equations (10) and (11) to solve these problems.

$$Y_{d,n}^* = \frac{Y_{d,n}}{Y_{d\max}} \quad (10)$$

$$Y_{c,n}^* = \frac{Y_{c,n}}{Y_{c\max}} \quad (11)$$

Where n provides the index of each point and $Y_{d,n}^*$ and $Y_{c,n}^*$ show normalized form of Y_d and Y_c. Results of normalization can be seen in Figure 9 and the last 2 columns of Table 10.

The manufacturing cost of each point in Figure 9 can be reliably estimated by Equation (12). Where P_h represents the cost to manufacture the customer's part based on inputs related to Y_c^* equal to one, and n indicates the index of each point.

$$P_n \approx P_h \times Y_{c,n}^* \quad (12)$$

[Figure 9]

Finally, the customer can choose each given point in Figure 9. For example, our customer has selected the 20th point with the coordinates (0.6305, 0.5987). The optimal input parameters for this case study are shown in Table 11. According to these input settings, the most satisfactory and suitable part has been manufactured for this customer. **[Table 11]**

This algorithm was tested on eight other customers to ensure its effectiveness. On a scale of 0-100, they expressed their satisfaction with the expected price and quality. The average result of 88.56 indicates the high efficiency of the proposed method.

4. Conclusion

This study aimed to optimize FDM 3D printing process parameters based on customers' demands. The investigation considered three response variables as outputs and eight process parameters as inputs. The experiments based on Taguchi L27 were designed and manufactured in two iterations. After obtaining S/N ratios, three full quadratic regression base equations for

output responses were generated and show that the layer thickness, infill density, print speed, number of shells, and infill pattern significantly affect the output responses.

According to the customer's demands, a quality function was defined, which is a weighted geometric average of dimensional accuracy and tensile strength. Following this, the quality and cost functions were used to define the fitness function. A Multi-objective optimization was done using NSGA II, and a two-dimensional optimal Pareto front was achieved and normalized. Then, the customer could select any point on the Pareto front that was more favorable to them according to their expectations. The most important innovations of this research are carrying out multi-objective optimization based on three outputs, presenting a range of optimal points instead of a single one, assigning the weights of outputs based on customer's demands, making visual sense by presenting the 2D optimal Pareto front, and having the potential of generalizing to other cases by presenting the normalized form of Pareto front.

Further studies can focus on other materials such as ABS and nylon, as well as other characteristics of FDM parts, including surface roughness, flexural strength, and compressive strength, covering a greater range of customer demands. Utilizing an artificial neural network or an adaptive neuro-fuzzy inference system in mathematical modeling has considerable potential to provide excellent results. Furthermore, the same approach could be applied to other AM technologies to make them more satisfactory for customers.

Nomenclature	
2D	Two-Dimensional
3D	Three-Dimensional
ABS	Acrylonitrile Butadiene Styrene
AM	Additive Manufacturing
CAD	Computer Aided Design
FDM	Fused Deposition Modeling
ID	Infill Density
IP	Infill Pattern
LT	Layer Thickness
NS	Number of Shells
NT	Nozzle Temperature
OR	Orientation
PLA	Polylactic Acid
PP	Print Position
PS	Print Speed
RSM	Response Surface Methodology
S/N	Signal/Noise

Reference

1. Parandoush, P. and Lin, D., "A review on additive manufacturing of polymer-fiber composites", *Compos. Struct.*, **182**, pp. 36–53 (2017).

2. Dizon, J. R. C., Espera, A. H., Chen, Q., et al., "Mechanical characterization of 3D-printed

polymers", *Addit. Manuf.*, **20**, pp. 44–67 (2018).

3. Wang, X., Jiang, M., Zhou, Z., et al., "3D printing of polymer matrix composites: A review and prospective", *Compos. Part B Eng.*, **110**, pp. 442–458 (2017).

4. Ngo, T. D., Kashani, A., Imbalzano, G., et al., "Additive manufacturing (3D printing): A review of materials, methods, applications and challenges", *Compos. Part B Eng.*, **143**, pp. 172–196 (2018).

5. Khan, R. U., Salamzadeh, Y., Iqbal, Q., et al., "The impact of customer relationship management and company reputation on customer loyalty: The mediating role of customer satisfaction", *J. Relatsh. Mark.*, **21**(1), pp. 1–26 (2022).

6. Meilatinova, N., "Social commerce: Factors affecting customer repurchase and word-of-mouth intentions", *Int. J. Inf. Manage.*, **57**, p. 102300 (2021).

7. Islam, T., Islam, R., Pitafi, A. H., et al., "The impact of corporate social responsibility on customer loyalty: The mediating role of corporate reputation, customer satisfaction, and trust", *Sustain. Prod. Consum.*, **25**, pp. 123–135 (2021).

8. Liu, X., Zhang, M., Li, S., et al., "Mechanical property parametric appraisal of fused deposition modeling parts based on the gray Taguchi method", *Int. J. Adv. Manuf. Technol.*, **89**(5), pp. 2387–2397 (2017).

9. Yaman, U., "Shrinkage compensation of holes via shrinkage of interior structure in FDM process", *Int. J. Adv. Manuf. Technol.*, **94**(5), pp. 2187–2197 (2018).

10. Raju, M., Gupta, M. K., Bhanot, N., et al., "A hybrid PSO–BFO evolutionary algorithm for optimization of fused deposition modelling process parameters", *J. Intell. Manuf.*, **30**(7), pp. 2743–2758 (2019).

11. Akbaş, O. E., Hıra, O., Hervan, S. Z., et al., "Dimensional accuracy of FDM-printed polymer parts", *Rapid Prototyp. J.* (2019).

12. Mendricky, R. and Fris, D., "Analysis of the accuracy and the surface roughness of fdm/fff technology and optimisation of process parameters", *Teh. Vjesn.*, **27**(4), pp. 1166–1173 (2020).

13. Dev, S. and Srivastava, R., "Optimization of fused deposition modeling (FDM) process parameters for flexural strength", *Mater. Today Proc.*, **44**, pp. 3012–3016 (2021).

14. Camposeco-Negrete, C., "Optimization of printing parameters in fused deposition modeling for improving part quality and process sustainability", *Int. J. Adv. Manuf. Technol.*, **108**(7), pp. 2131–2147 (2020).

15. Ramesh, M. and Panneerselvam, K., "Mechanical investigation and optimization of parameter selection for Nylon material processed by FDM", *Mater. Today Proc.*, **46**, pp. 9303–9307 (2021).

16. Mohamed, O. A., Masood, S. H., and Bhowmik, J. L., "Modeling, analysis, and optimization of dimensional accuracy of FDM-fabricated parts using definitive screening design and deep learning feedforward artificial neural network", *Adv. Manuf.*, **9**(1), pp.

115–129 (2021).

17. Haghshenas Gorgani, H., Korani, H., Jahedan, R., et al., "A Nonlinear Error Compensator for FDM 3D Printed Part Dimensions Using a Hybrid Algorithm Based on GMDH Neural Network", *J. Comput. Appl. Mech.*, **52**(3), pp. 451–477 (2021).

18. Rezaeian, P., Ayatollahi, M. R., Nabavi-Kivi, A., et al., "Effect of printing speed on tensile and fracture behavior of ABS specimens produced by fused deposition modeling", *Eng. Fract. Mech.*, **266**, p. 108393 (2022).

19. Sandhu, G. S., Boparai, K. S., and Sandhu, K. S., "Influence of slicing parameters on selected mechanical properties of fused deposition modeling prints", *Mater. Today Proc.*, **48**, pp. 1378–1382 (2022).

20. Tosto, C., Tirillò, J., Sarasini, F., et al., "Fused Deposition Modeling Parameter Optimization for Cost-Effective Metal Part Printing", *Polymers (Basel).*, **14**(16), p. 3264 (2022).

21. Gorgani, H. H., "Improvements in teaching projection theory using failure mode and effects analysis (FMEA)", *J. Eng. Appl. Sci.*, **100**(1), pp. 37–42 (2016).

22. Haghshenas Gorgani, H., Jahazi, A., Jahantigh Pak, A., et al., "Optimization of Wirecut EDM machine settings in order to achieve maximum customer satisfaction", in the 30th annual international conference of Iranian society of mechnical engineers (2022).

23. Natrayan, L. and Kumar, M. S., "An integrated artificial neural network and Taguchi approach to optimize the squeeze cast process parameters of AA6061/Al2O3/SiC/Gr hybrid composites prepared by novel encapsulation feeding technique", *Mater. Today Commun.*, **25**, p. 101586 (2020).

24. Rangaswamy, H., Sogalad, I., Basavarajappa, S., et al., "Experimental analysis and prediction of strength of adhesive-bonded single-lap composite joints: Taguchi and artificial neural network approaches", *SN Appl. Sci.*, **2**(6), pp. 1–15 (2020).

25. Haghshenas Gorgani, H. and Jahantigh Pak, A., "A genetic algorithm based optimization method in 3D solid reconstruction from 2D multi-view engineering drawings", *J. Comput. Appl. Mech.*, **49**(1), pp. 161–170 (2018).

List of captions:

No.	Caption
Table 1	Levels of input parameters
Table 2	List of experiments designed by L27 Taguchi orthogonal array
Table 3	Summary of experimental data
Table 4	Response table of S/N ratios for tensile strength
Table 5	Response table of S/N ratios for dimensional accuracy
Table 6	Response table of S/N ratios for production cost

Table 1. Levels of input parameters

Parameter	Level 1	Level 2	Level 3
Orientation (Deg)	0	45	90
Layer Thickness (mm)	0.06	0.18	0.27
Infill Density (%)	10	30	50
Print Position	Right (1)	Center (2)	Left (3)
Nozzle Temperature (℃)	190	205	220
Print Speed (mm/s)	30	42	55
Number of Shell	2	3	4
Infill Pattern	Grid (1)	Lines (2)	Triangles (3)

Table 2. List of experiments designed by L27 Taguchi orthogonal array

Exp. No.	Orientation (Deg)	Layer Thickness (mm)	Infill Density (%)	Print Position	Nozzle Temp. (℃)	Print Speed (mm/s)	Number of Shell	Infill Pattern
1	0	0.06	10	1	190	30	2	1
2	0	0.06	10	1	205	42	3	2
3	0	0.06	10	1	220	55	4	3
4	0	0.18	30	3	190	30	2	2
5	0	0.18	30	3	205	42	3	3
6	0	0.18	30	3	220	55	4	1
7	0	0.27	50	2	190	30	2	3
8	0	0.27	50	2	205	42	3	1
9	0	0.27	50	2	220	55	4	2
10	45	0.06	30	2	190	42	4	1
11	45	0.06	30	2	205	55	2	2
12	45	0.06	30	2	220	30	3	3
13	45	0.18	50	1	190	42	4	2

14	45	0.18	50	1	205	55	2	3
15	45	0.18	50	1	220	30	3	1
16	45	0.27	10	3	190	42	4	3
17	45	0.27	10	3	205	55	2	1
18	45	0.27	10	3	220	30	3	2
19	90	0.06	50	3	190	55	3	1
20	90	0.06	50	3	205	30	4	2
21	90	0.06	50	3	220	42	2	3
22	90	0.18	10	2	190	55	3	2
23	90	0.18	10	2	205	30	4	3
24	90	0.18	10	2	220	42	2	1
25	90	0.27	30	1	190	55	3	3
26	90	0.27	30	1	205	30	4	1
27	90	0.27	30	1	220	42	2	2

Table 3. Summary of experimental data

Exp. No.	Specimen Width (mm)				Mass (g)		Printing time (s)	Ultimate Tensile Force (N)	
	First Specimen		Second Specimen		First Specimen	Second Specimen		First Specimen	Second Specimen
1	19.02	19.01	19.02	18.95	10.2	10.3	25285	2162	2159
2	19.04	18.98	19.08	18.99	11	11.1	19797	2420	2277
3	19.01	18.92	18.89	19.08	11.8	11.6	16638	2634	2767
4	19.07	19.23	19.24	19.16	12.7	12.6	11213	2346	2244
5	19.22	19.18	19.18	19.26	13.3	13.3	8570	2314	2005
6	19.25	19.21	19.19	19.26	14.1	14.1	6874	2888	2930
7	19.28	19.42	19.58	19.29	15.1	15	9285	2268	2015
8	19.36	19.21	19.22	19.29	15.6	15.6	6824	2783	2172
9	19.23	19.36	19.66	19.4	16.1	16.1	5474	3073	3048
10	19.13	19.07	19.13	19.05	13.8	13.8	24954	2817	2357
11	19.15	19.08	19.16	19.12	13	13	18145	2185	2480
12	19.12	19.14	19.16	19.21	13.9	13.8	33708	2586	2200
13	19.28	19.2	19.31	19.21	16.2	16.2	10265	3219	3150
14	19.36	19.34	19.36	19.42	15.4	15.4	7701	2577	2358
15	19.37	19.33	19.4	19.31	16	16.1	13817	2727	2844
16	19.25	19.26	19.29	19.28	10.9	10.9	5293	2349	2377
17	19.25	19.26	19.29	19.22	9.6	9.6	3632	1876	1837
18	19.23	19.23	19.24	19.22	10.4	10.5	6763	2119	2208
19	19.13	19.6	19.05	19.07	15.9	15.7	22234	2848	2692
20	19.03	19.12	19.08	19.07	16.9	16.8	40115	3064	3052
21	19.18	19.1	19.11	19.1	15.7	15.6	28315	2432	2330
22	19.24	19.14	19.22	19.21	10.4	10.4	5670	2339	2239
23	19.12	19.15	19.14	19.12	11.2	11.2	10423	2549	2471
24	19.15	19.12	19.11	19.15	9.8	9.7	6662	1899	1869
25	19.28	19.27	19.22	19.21	12.6	12.5	4726	2203	2188
26	19.32	19.2	19.26	19.27	13.5	13.5	8456	2647	2572
27	19.29	19.28	19.32	19.26	12.2	12.2	5716	2210	2190

Table 4. Response table of S/N ratios for tensile strength

Level	OR	LT	ID	PP	NT	PS	NS	IP
1	67.90	68.00	67.00	67.95	67.69	67.75	66.78	67.79

2	67.73	67.85	67.60	67.68	67.73	67.63	67.67	68.02
3	67.64	67.42	68.68	67.65	67.85	67.90	68.83	67.46
Delta	0.26	0.58	1.68	0.30	0.17	0.27	2.05	0.56
Rank	7	3	2	5	8	6	1	4
Impact	4.43%	9.88%	28.62%	5.11%	2.90%	4.60%	34.92%	9.54%

Table 5. Response table of S/N ratios for dimensional accuracy

Level	OR	LT	ID	PP	NT	PS	NS	IP
1	18.81	24.31	20.62	18.33	16.71	16.49	16.15	16.88
2	13.35	13.36	14.51	14.51	16.44	16.65	15.94	16.19
3	16.38	10.87	13.41	15.71	15.40	15.41	16.46	15.47
Delta	5.46	13.43	7.20	3.82	1.31	1.24	0.52	1.41
Rank	3	1	2	4	6	7	8	5
Impact	15.88%	39.05%	20.94%	11.11%	3.81%	3.60%	1.51%	4.1%

Table 6. Response table of S/N ratios for production cost

Level	OR	LT	ID	PP	NT	PS	NS	IP
1	-34.40	-40.75	-32.87	-34.45	-34.45	-36.67	-34.08	-34.35
2	-34.48	-32.65	-34.55	-34.46	-34.45	-34.25	-34.48	-34.41
3	-34.50	-29.98	-35.96	-34.48	-34.48	-32.46	-34.82	-34.62
Delta	0.09	10.77	3.09	0.03	0.04	4.20	0.73	0.28
Rank	6	1	3	8	7	2	4	5
Impact	0.46%	56.01%	16.07%	0.16%	0.21%	21.84%	3.80%	1.46%

Table 7. Analysis of variance response for tensile strength

Source	DF	Adj SS	Adj MS	F-	P-
Model	7	2917191	416742	33.00	0.000
Linear	4	2722785	680696	53.91	0.000
LT	1	95689	95689	7.58	0.013
ID	1	1028621	1028621	81.46	0.000
NS	1	1539135	1539135	121.89	0.000
IP	1	59340	59340	4.70	0.043
Square	2	134364	67182	5.32	0.015

ID×ID	1	44204	44204	3.50	0.077
IP×IP	1	90160	90160	7.14	0.015
2-Way interaction	1	34511	34511	2.73	0.115
LT×ID	1	34511	34511	2.73	0.115
Error	19	239921	12627		
Total	26	3157112			

Table 8. Analysis of variance response for dimensional error

Source	DF	Adj SS	Adj MS	F-	P-
Model	2	0.26921	0.134603	55.72	0.000
Linear	2	0.26921	0.13460	55.72	0.000
LT	1	0.21112	0.211123	87.40	0.000
ID	1	0.05808	0.058084	24.04	0.000
Error	24	0.05798	0.002416		
Total	26	0.32718			

Table 9. Analysis of variance response for production cost

Source	DF	Adj SS	Adj MS	F-	P-
Model	9	76.8704	8.5412	203.07	0.000
Linear	4	64.0999	16.0250	380.99	0.000
LT	1	50.9662	50.9662	1211.72	0.000
ID	1	4.3654	4.3654	103.79	0.000
PS	1	8.4071	8.4071	199.88	0.000
NS	1	0.3222	0.3222	7.66	0.013
Square	2	5.6615	2.8308	67.30	0.000
LT*LT	1	5.4277	5.4277	129.04	0.000
PS*PS	1	0.2338	0.2338	5.56	0.031
2-Way Interaction	3	4.4093	1.4698	34.94	0.000
LT*ID	1	1.4338	1.4338	34.09	0.000
LT*PS	1	2.6501	2.6501	63.01	0.000
ID*PS	1	0.3254	0.3254	7.74	0.013
Error	17	0.7150	0.0421		
Total	26	77.5854			

Table 10. Response table for optimal Pareto front of the case study

Index	Inputs					Outputs		Normalized Outputs	
	LT	ID	PS	NS	IP	Y_c	Y_d	Y_c^*	Y_d^*
1	0.219	12.02	52.66	2	2	0.7893	0.00432	0.2463	1.000
2	0.194	11.54	52.35	2	2	0.8381	0.00406	0.2615	0.9413
3	0.214	10.84	52.99	3	2	0.9135	0.00390	0.2850	0.9030
4	0.193	11.48	52.78	3	2	0.9732	0.00371	0.3037	0.8606
5	0.174	10.35	53.16	3	2	1.0613	0.00352	0.3311	0.8147
6	0.185	10.42	53.28	4	2	1.1276	0.00336	0.3518	0.7775
7	0.174	10.82	53.22	4	2	1.2054	0.00327	0.3761	0.7565
8	0.166	10.26	53.62	4	2	1.2570	0.00318	0.3922	0.7365
9	0.164	10.46	52.98	4	2	1.2870	0.00317	0.4015	0.7333
10	0.159	10.26	52.92	4	2	1.3269	0.00312	0.4140	0.7226
11	0.154	10.32	53.36	4	2	1.3804	0.00306	0.4307	0.7100
12	0.148	10.34	53.07	4	2	1.4503	0.00301	0.4525	0.6972
13	0.145	10.25	53.36	4	2	1.4752	0.00298	0.4603	0.6904
14	0.142	10.31	53.19	4	2	1.5236	0.00295	0.4754	0.6826
15	0.138	10.19	53.36	4	2	1.5661	0.00291	0.4886	0.6730
16	0.132	10.34	53.30	4	2	1.6543	0.00285	0.5162	0.6593
17	0.128	10.34	53.01	4	2	1.7308	0.00280	0.5400	0.6478
18	0.121	10.24	53.30	4	2	1.8258	0.00272	0.5697	0.6298
19	0.115	10.34	53.28	4	2	1.9383	0.00265	0.6048	0.6132
20	0.110	10.29	53.50	4	2	2.0206	0.00258	0.6305	0.5987
21	0.107	10.18	53.39	4	2	2.0844	0.00254	0.6503	0.5883
22	0.104	10.20	52.82	4	2	2.1517	0.00251	0.6714	0.5813
23	0.101	10.20	53.18	4	2	2.2137	0.00246	0.6907	0.5698
24	0.098	10.27	53.22	4	2	2.2664	0.00243	0.7071	0.5624
25	0.094	10.27	53.44	4	2	2.3382	0.00237	0.7295	0.5502
26	0.092	10.33	53.24	4	2	2.3891	0.00235	0.7454	0.5444
27	0.088	10.18	53.35	4	2	2.4702	0.00228	0.7707	0.5293
28	0.085	10.36	53.58	4	2	2.5310	0.00225	0.7897	0.5210
29	0.083	10.33	53.41	4	2	2.6021	0.00220	0.8119	0.5105
30	0.081	10.27	53.53	4	2	2.6331	0.00218	0.8215	0.5041
31	0.080	10.17	52.98	4	2	2.6705	0.00216	0.8332	0.5005
32	0.078	10.26	53.45	4	2	2.6995	0.00213	0.8423	0.4940
33	0.076	10.21	53.40	4	2	2.7626	0.00209	0.8620	0.4833
34	0.071	10.19	53.43	4	2	2.8813	0.00200	0.8990	0.4632
35	0.067	10.17	53.40	4	2	2.9928	0.00192	0.9338	0.4441
36	0.066	10.18	52.94	4	2	3.0320	0.00191	0.9460	0.4413
37	0.065	10.16	52.84	4	2	3.0643	0.00188	0.9561	0.4363
38	0.064	10.21	52.87	4	2	3.0996	0.00186	0.9671	0.4306
39	0.062	10.18	52.76	4	2	3.1497	0.00182	0.9827	0.4220
40	0.060	10.16	52.69	4	2	3.2050	0.00178	1.0000	0.4121

Table 11. The optimal setting, according to the customer's requirements

Layer Thickness	Infill Density	Print Speed	Number of Shells	Infill pattern
0.11 (mm)	10.3%	53.5 (mm/s)	4	Liners

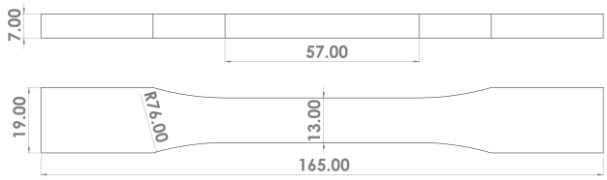

Figure 1. Test specimen type I (dimensions are in millimeters)

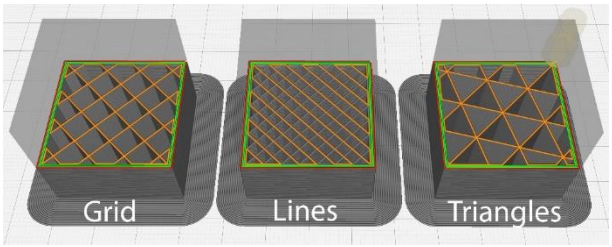

Figure 2. Infill patterns that are used in experiments (Infill density is constant in all three cubes)

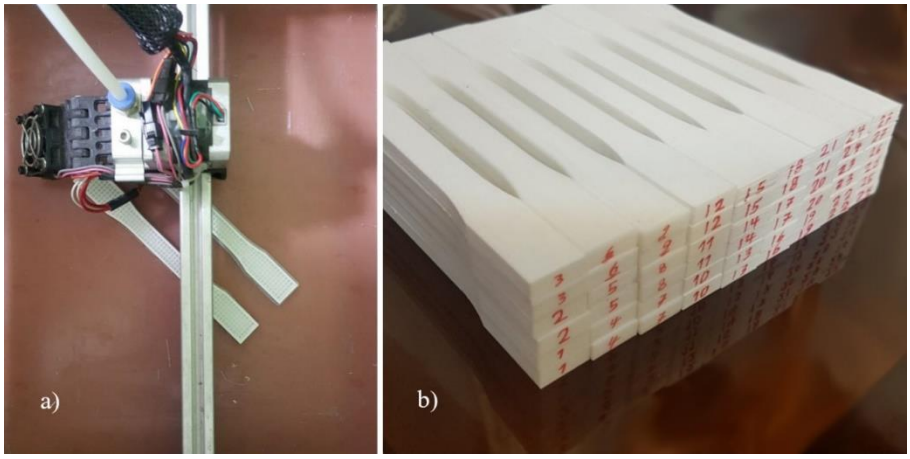

Figure 3. a) FDM 3D printing of the specimen on Quantum 2025 and b) all specimens printed based on the designed experiments

Figure 4. The loaded specimen in the tensile strength test

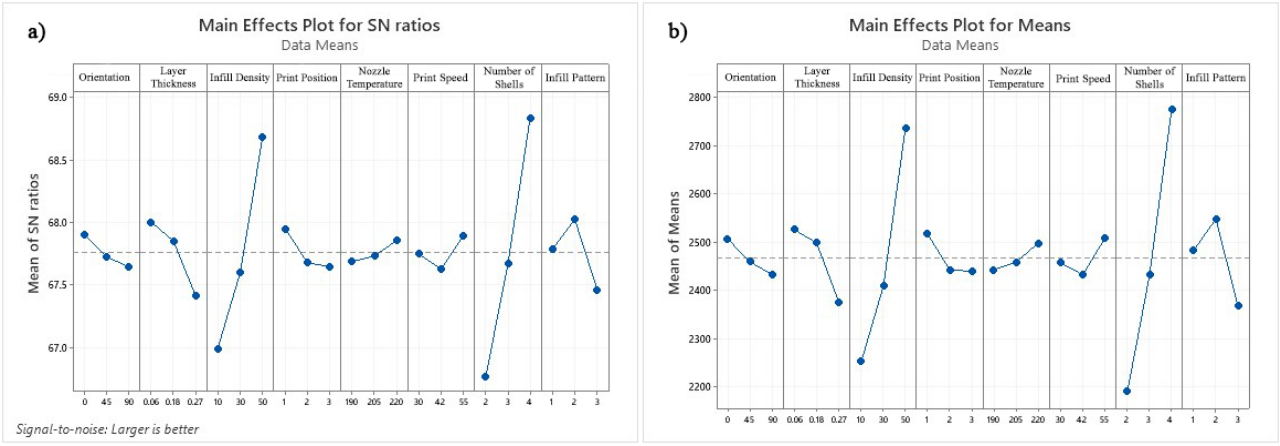

Figure 5. Main effects plot of a) S/N ratios and b) means for tensile strength

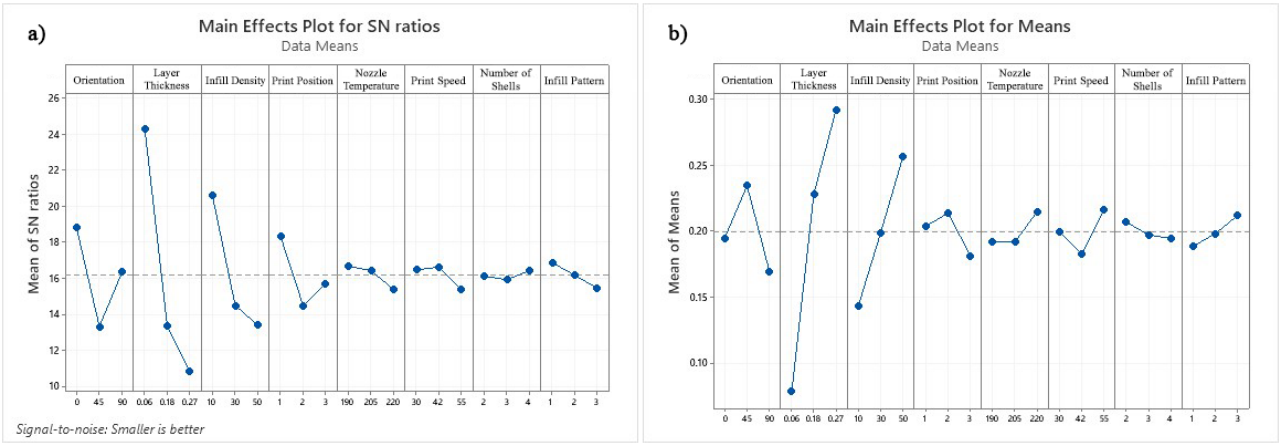

Figure 6. Main effects plot of a) S/N ratios and b) means for dimensional accuracy

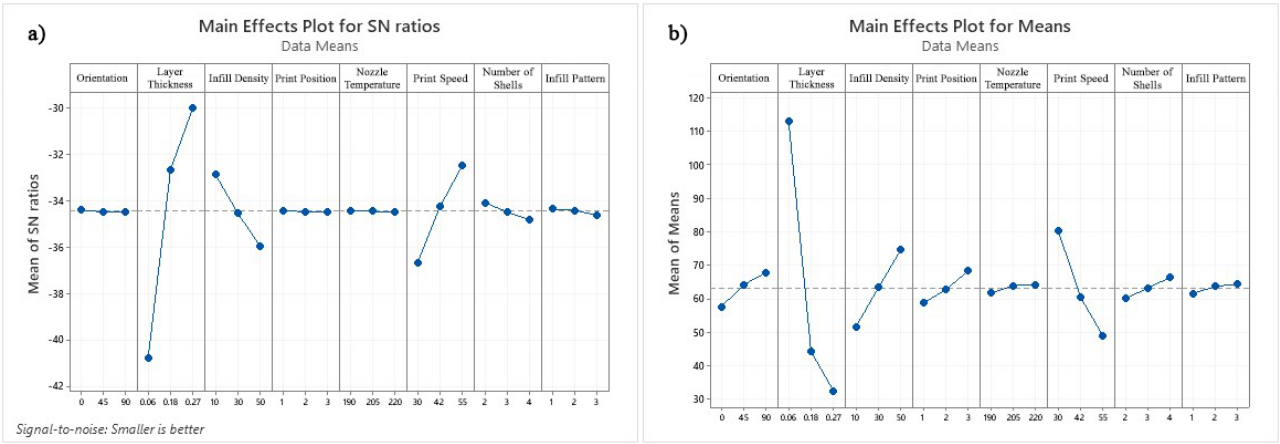

Figure 7. Main effects plot of a) S/N ratios and b) means for production cost

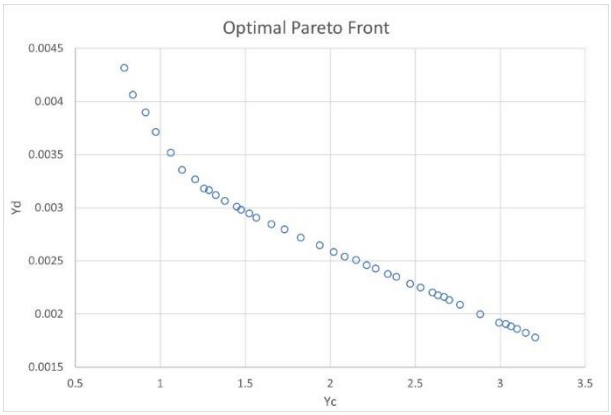

Figure 8. Optimal Pareto front obtained for the fitness function based on the customer demands

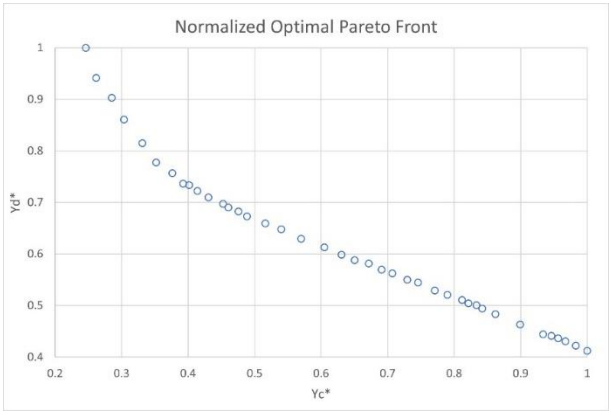

Figure 9. Normalized optimal Pareto front

Mohammad Ali Zonoobi obtained his Bachelor of Science in Mechanical Engineering from Sharif University of Technology. His research interests encompass the areas of additive manufacturing, mechatronics, product development, and advanced computer-aided design.

Mohammad Ali Zonoobi obtained his Bachelor of Science in Mechanical Engineering from Sharif University of Technology. He has experience of working on various industrial and research projects. His research interests encompass the areas of additive manufacturing, mechatronics, product development, and advanced computer-aided design.

Hamid Haghshenas Gorgani Graduated in mechanical engineering, applied design from Sharif University of Technology. He has been a member of the faculty at Sharif University of Technology since 2011. His research areas are plastic injection mold design, reverse engineering,

design optimization with metaheuristic algorithms, design data processing, and engineering education methods.

Dorin Javaherneshan is a dual M.Sc. degree student at Aalto University and Chalmers University of Technology in the field of Sustainable Energy Engineering. She received her B.Sc. degree in Mechanical Engineering from Sharif University of Technology. Her research interests relevant to this research, are economic assessment, market analysis, and optimization methods.